Time-resolved structural dynamics of the out-of-equilibrium charge density wave phase transition in GdTe 3

I González-Vallejo, V L R Jacques, D Boschetto, G Rizza, A Hadj-Azzem, Jérôme Faure, D Le Bolloc'H

Time-resolved structural dynamics of the out-of-equilibrium charge density wave phase transition in $GdTe_3$

I. González-Vallejo,[1,2,a] V. L. R. Jacques,[1] D. Boschetto,[2] G. Rizza,[3] A.Hadj-Azzem,[4] J. Faure,[2,b] and D. Le Bolloc'h[1,c]

[1)] *LPS, Université Paris Saclay, CNRS, Orsay, France*

[2)] *LOA, ENSTA ParisTech, CNRS, Ecole polytechnique, Palaiseau, France*[d)]

[3)] *LSI, CNRS, Ecole Polytechnique, Institute Polytechnique de Paris, France*

[4)] *CNRS, Institut Néel, 38042 Grenoble, France*

(Dated: 31 August 2021)

We use ultrafast electron diffraction (UED) to study the out-of-equilibrium dynamics of the charge density wave (CDW) phase transition in $GdTe_3$, a quasi-two-dimensional compound displaying a unidirectional CDW state. Experiments were conducted at different incident fluences and different initial sample temperatures below T_c. We find that following photo-excitation, the system undergoes a non-thermal ultrafast phase transition that occurs in out-of-equilibrium conditions. The intrinsic crystal temperature was estimated at each time delay from the atomic thermal motion which affects each Bragg peak intensity via the Debye Waller factor. Assuming an isotropic harmonic potential, we estimate the out-of-equilibrium temperature T_{qe} as a function of the laser fluence. We then relate the recovery time constants and correlation lengths as a function of T_{qe}. The charge density wave is suppressed in less than a picosecond and recovers the long range order with increasing recovery times with increasing fluences and increasing initial temperatures. The measured relaxation times are discussed in terms of the Rothwarf-Taylor model. If indeed, the recovery time increases for initial temperatures closer to T_c in agreement with the model, this one cannot however explain the slowness of the system to return to its ground state. In addition, the transient CDW phase recently observed along the transverse direction in $LaTe_3$ and $CeTe_3$ is not observed in $GdTe_3$.

I. INTRODUCTION

The understanding of the microscopic mechanisms behind phase transitions in systems displaying couplings between different degrees of freedom (charge, lattice, spin and orbitals) has become a key topic in condensed matter physics. These systems, like superconductors or materials displaying spin or charge density waves (CDW), are particularly sensitive to ultra-fast laser pulses that reveal the interplay between the different degrees of freedom and the competition between phases. A good example of such competitions has been studied in the case of the cuprates[1,2]. However, CDW systems are also of great interest and pump-probe experiments on these materials have revealed, in recent years, complex metastable states linked to electron-phonon coupling. In the quasi-1D systems and in the weak coupling approach, the system becomes unstable below T_c. The electronic structure undergoes a band gap opening at the Fermi wave vector induced by a periodic lattice distortion associated to a soft phonon and leading to a modulated electronic wave function[3]. Less understood is the formation of the CDW state in 2D materials[4,5], in which tight-binding models describing partial Fermi surface nesting could only be applied to some systems, as Rare-Earth tritellurides[6,7].

The ultrafast dynamics of this phase transition has recently been studied in several CDW materials with pump-probe experiments. A strong optical excitation triggers coherent collective excitations[8,9], involving phase and amplitude fluctuations[10,11], and leads to the melting of charge and orbital states[12,13] or influences the type of transition between CDW states[14,15].

The mechanism of the phase recovery has recently attracted particular attention[16,17]. Among many possible scenarii, the role of topological defects, like CDW dislocations, has been widely invoked to explain the slow dynamics of the CDW recovery after photo-excitation[18] either by optical pump-probe spectroscopy[19,20] or by time-resolved diffraction[11,18,21,22]. Photo-induced topological defects have also been invoked to explain the emergence of an unexpected and astonishing transient CDW state that was never observed at equilibrium conditions, as recently discovered in $LaTe_3$[23] and $CeTe_3$[22]. In other diffraction studies however, the loss of long-range order after the laser pulse has not been observed as in $La_{1.75}Sr_{0.25}NiO_4$[10] or in $SmTe_3$[24].

Ultrafast structural probes such as electron or X-ray diffraction[25–28] are the ideal tools to specifically probe CDWs since the periodic lattice distortion associated to the CDW gives rise to new satellite reflections in the diffraction pattern. This is particularly true in the case of layered transition-metal dichalcogenides since the satellite reflections intensity are strong compared to most CDW systems.

Rare-earth tritellurides (RTe_3, with R standing for the rare-earth element), are a family of compound displaying a rich phase diagram. The RTe_3 systems may stabilize two types of one-dimensional CDWs which appear at different temperatures and have perpendicular wave vector to each other and superconductivity under pressure. All these phases are strongly affected by chemical substitution of the rare earth element[29]. As an illustration, the transition temperatures appearing along

[a)] Present address: Max-Born-Institut für Nichtlineare Optik und Kurzzeitspektroskopie, 12489 Berlin, Germany

[b)] Electronic mail: jerome.faure@ensta-paris.fr

[c)] Electronic mail: david.le-bolloch@u-psud.fr

[d)] Electronic mail: isabel.gonzalezvallejo@mbi-berlin.de

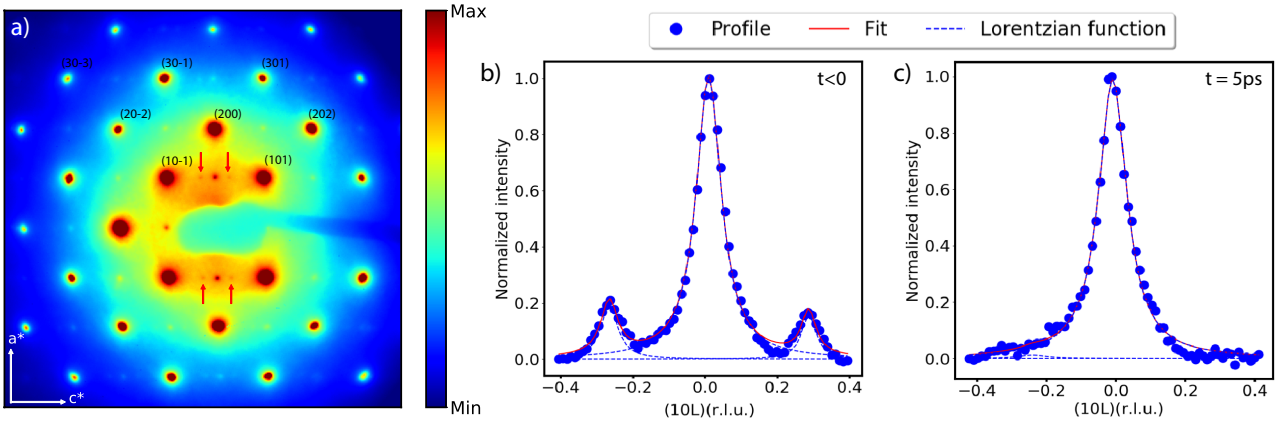

FIG. 1. a) Diffraction pattern of the $GdTe_3$ thin films at equilibrium conditions for $T_i = 155$ K in (010) plane. The red arrows point to the satellite peaks associated to the CDW. Intensity profiles along the c^* direction (given in reciprocal lattice unit) with an incident fluence of F= 3.5 mJ/cm^2 before pump arrival (b), and after pump arrival at t=5 ps (c). The red solid line is the fit obtained from three single Lorentzian profiles (blue dashed lines).

the c direction can switch from $T_c = 240$ K for $TmTe_3$, to 377 K for $GdTe_3$, or 670 K for $LaTe_3$.

In this paper, we present time-resolved electron diffraction experiments performed on thin $GdTe_3$ films, thereby extending the exploration of the RTe_3 family, especially the previous studies performed on $LaTe_3$[18] and $CeTe_3$[11,22] by pump-probe electron diffraction. The results are organized as follows: we first present details on the experimental methods and the sample in section II. In section III A we show an analysis of the dynamics of the main Bragg reflections, leading to an estimation of the lattice temperature and showing the existence of a quasi-equilibrium state where the lattice is thermalized. Section III B focuses on the temporal dynamics of the satellite reflections with a particular emphasis on the role of the initial temperature. Indeed, as the initial temperature approaches T_c, a large increase of the recovery time is observed. This effect is discussed in terms of the Rothwarf-Taylor (RT) model. Finally, the absence of the perpendicular transient CDW phase in $GdTe_3$ is discussed.

II. EXPERIMENTAL DETAILS

A. Experimental Setup

Our experimental setup relies on a compact DC electron gun and a commercial Ti:Sapphire amplifier which delivers 35 fs pulses centered at a wavelength of 800 nm with an energy of 1 mJ at a repetition rate of 1 kHz. The electron bunches are generated by the photoelectric effect after back-illumination by the third harmonic of the laser source ($\lambda_{3\omega} = 266\,nm$) on a 20 nm gold film coated on the photocathode. The experiments were performed with 41 keV electron energy and 10000 electrons per bunch. For this beam charge, the bunch duration is 1-1.5 ps with an electron beam spot size of 300 μm at the sample position. Most data were taken in this high-charge and "long-pulse" duration regime in order to optimize the signal-to-noise ratio. Some data were also taken with lower charge (1000-2000 electron per bunch), resulting in better resolution of ~ 300 fs. Bunch durations were estimated by simulating beam dynamics in the electron gun using the general particle tracer (GPT) code[30]. The experimental setup works in transmission geometry with the pump beam impinging the sample close to normal incidence and with a transverse FWHM of 750 μm. By measuring the laser beam profile at the virtual sample position, the incident fluence can be obtained with a typical systematic error of ± 0.2mJ/cm^2.

The signal from the diffracted electron beam is amplified by a multi-channel plate and detected by a P43 phosphor plate; the diffraction patterns are recorded with an air-cooled CCD camera after demagnification with an spatial resolution of $39\times39\mu$m^2 per pixel. The time delay between pump and probe pulses is set by a mechanical delay line. At each time delay, the diffraction patterns were collected with an exposure time of 3 s and the final diffraction pattern results from an average over 5 images. The total measured temporal range covers the first 140 ps after pump beam arrival, allowing the study of thermal processes occurring tens of picosecond after photo-excitation. The sample cooling system consists of a liquid nitrogen cold finger attached to the copper sample holder by a copper braid allowing to reach a minimum temperature of 155 K.

B. Sample description

RTe_3 are quasi-two-dimensional materials that have attracted great interest due to their properties[29,31]. All compounds belonging to this family present at least one unidirectional CDW state for critical temperatures between 110 K and 670 K, a value that is set by the chemical pressure induced by the R ion[31–33]. Their unit cell presents a weakly orthorhombic (quasi-tetragonal) symmetry, belonging to the *Cmcm* space group. It consists of RTe slabs sandwiched between Te single layers and stacked along the b axis, which confers the quasi

2D character. The lattice parameters are $b \gg a \gtrsim c$ with a and c defining the in-plane parameters in the Te layers. The small anisotropy between a and c leads to different nesting conditions and favors the emergence of the periodic lattice modulation along the c axis at higher temperatures[23,34]. The heaviest compounds of the family present a higher chemical pressure favoring the reduction of the anisotropy between the a and c lattice parameters and leading to the emergence of a second CDW along the a crystallographic axis at lower temperatures. The system we study here, $GdTe_3$, presents a unidirectional CDW along the c axis below the critical temperature $T_c \sim 377$ K. We were thus able to probe this system starting from two initial temperatures below T_c: $T_i = 155$ K and at room temperature.

Single crystals were grown by a self-flux technique under purified argon atmosphere in a sealed quartz tube. The mixture containing Gd and Te is first heated at sufficiently high temperature for several days before cooling down and then quenched in air to room temperature[35]. The $GdTe_3$ thin films with $50\,\text{nm} \pm 2\,\text{nm}$ thickness and a surface of $\sim 500\,\mu\text{m} \times 500\,\mu\text{m}$ were prepared by ultramicrotomy from a bulk sample. They were then deposited on a 200 mesh copper TEM grid.

III. RESULTS

A typical diffraction pattern from the $GdTe_3$ thin film is presented in figure 1a). The diffraction pattern was collected at equilibrium conditions with 41 keV electron energy at 155 K. As expected, the main $(h+l) = 2n$ Bragg reflections show a quasi-squared symmetry with $a^* \sim c^*$ (a/c=0.9976)[34]). Note that $(h+l) = 2n+1$ are forbidden reflections in the *Cmcm* space group. These reflections are nevertheless present in our diffraction patterns which has been could be ascribed to disordered twins along b and sample bending[36]. The satellite reflections (pointed by the red arrows in the figure) appear along the c^* direction at $(\pm 1, 0, \pm\delta)$ with $\delta \sim 2/7$. In figures 1b) and 1c) we plot the intensity profiles along the c^* axis showing the two satellite reflections located on both sides of the (100) Bragg reflection before pump arrival and their disappearance t=5 ps after the laser pulse excitation with an incident fluence of $3.5\,\text{mJ/cm}^2$. The disappearance of the satellite reflections indicates the loss of long range order of the periodic lattice modulation. However, as we will see in the following sections, this disappearance does not correspond to the equilibrium disordered phase, but to an athermal out-of-equilibrium phase, occurring when the sample temperature does not exceed the critical temperature T_c and before the lattice is fully thermalized.

A. Dynamics of the main Bragg reflections and lattice temperature estimation

We first consider the intensity changes of the main Bragg reflections as a function of pump-probe delay. The intensity of a Bragg peak is estimated by integrating the diffracted signal over a small region of interest (ROI) around the corresponding peak. Figure 2 displays the relative intensity changes of the $(h+l) = 2n$ Bragg reflections averaged over thirty peaks.

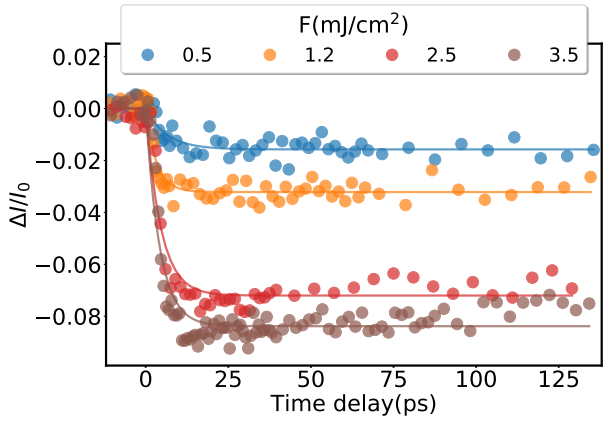

FIG. 2. Circles: relative intensity changes of the Bragg peaks integrated intensity as a function of pump-probe delay for four different fluences. Each curve is the result of averaging over 30 Bragg peaks. The initial sample temperature is $T_i = 155$ K. The solid lines represent the single exponential fits to the data.

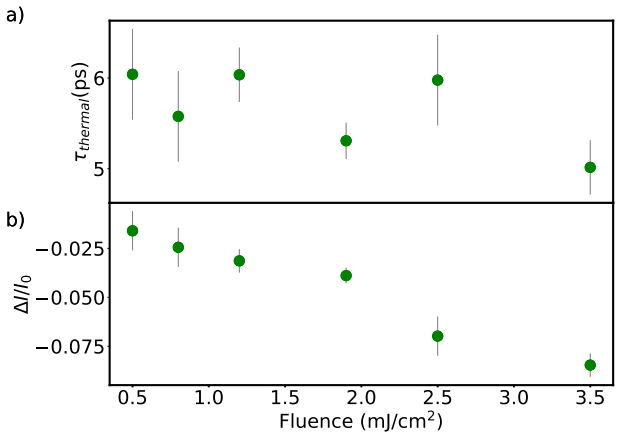

FIG. 3. a) Decay times $\tau_{thermal}$ extracted from the fits of figure 2. b) Decay amplitude of the Bragg intensity $\Delta I/I_0$ measured after the system has reached the quasi-equilibrium state. Both graphs are represented as a function of the incident fluence in the range $0.5 - 3.5\,\text{mJ/cm}^2$ with T_i=155K.

The evolution of the relative intensity is plotted as a function of time delay in figure 2 for different fluences. The curves are well described by a single exponential decay: $\Delta I/I_0 = A(1 - e^{-t/\tau_{thermal}}) \times H(t)$, where I_0 is the equilibrium peak intensity (without pump), $\tau_{thermal}$ the decay time representing the thermalization time, $A = \Delta I(t \gg \tau_{thermal})/I_0$ the amplitude of the decay at long times and $H(t)$ is the Heaviside function centered at $t = 0$ ps. The decay times $\tau_{thermal}$ and decay amplitudes A extracted from the fits are plotted in figure 3. The decay time of the Bragg peaks is typically $\tau_{thermal} = 5$-6 ps and does not significantly depend on the incident fluence (see figure 3 a)). The intensity reaches a steady value after ~20ps

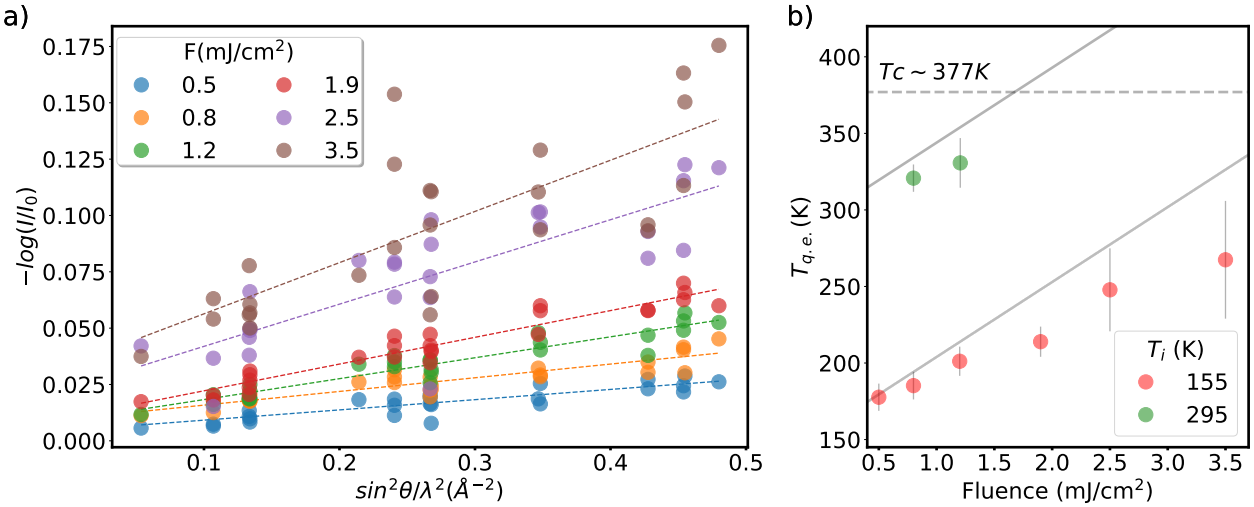

FIG. 4. a) Logarithm of the intensity ratio $-\log(I/I_0)$ after the quasi-equilibrium is reached ($t \simeq 75$ ps), as a function of $(Q/4\pi)^2 = sin^2\theta/\lambda^2$. As expected from Debye-Waller theory, $\ln(I/I_0)$ vs. Q^2 follows a linear trend. Dashed lines are linear fits to the data. b) Quasi-equilibrium lattice temperature $T_{q.e.}$ versus incident fluence extracted from the fits of a). Red (green) circles are estimated from the Debye-Waller analysis and correspond to initial temperature of $T_i = 155$ K ($T_i = 295$ K). The gray lines are temperature estimations from laser energy absorption. The dashed line marks the transition temperature of $GdTe_3$.

and remains constant for the whole scan duration, i.e. about 140 ps. Longer scans up to 2ns did not reveal extra relaxation processes.

The fact that a constant intensity ratio persists over nanoseconds, without reaching the equilibrium state, infers that the main lattice reaches a *quasi-equilibrium* state. Note that this pump-probe process is intrinsically reversible with our 1kHz laser repetition rate. The sample does return to the thermodynamic equilibrium between two laser pulses but the accessible time domain does not allow us to observe the complete relaxation. We can estimate that the quasi-equilibrium state persists over several nanoseconds as thermal conduction occurs, through acoustic phonons, on a longer time scale for these free-standing samples.

Contrary to the behavior of the thermalization time $\tau_{thermal}$, the Bragg peak intensity strongly depends on fluence. This can be explained by a pure thermal effect since higher fluences lead to higher lattice temperatures which increases the thermal mean-squared atomic displacements and decreases Bragg peak intensities through the Debye-Waller factor. For an isotropic medium in an harmonic potential, the intensity can be written as:

$$I \propto I_0\, e^{-2M} \tag{1}$$

where $2M = Q_{hkl}^2\langle u^2\rangle/3 = \left(\frac{4\pi}{\lambda}\right)^2 sin^2\theta\langle u^2\rangle/3$ with Q_{hkl} the scattering wave vector, $\langle u^2\rangle$ is the mean-squared amplitude of the atomic displacement, λ the de Broglie electron wavelength and θ the scattering angle. By adding a few assumptions (see Supplementary Material for more details), the parameter M can then be related to the lattice temperature T, the Debye temperature Θ_D and the Debye integral $\varphi(x)$[37] as follows:

$$2M = \left(\frac{\sin\theta}{\lambda}\right)^2 \frac{12h^2}{mk_B\Theta_D}\left(\frac{\varphi(\Theta_D/T)}{\Theta_D/T}\right)$$

Figure 4a) shows the logarithm of the intensity ratio $-\ln(I/I_0)$ after the sample has reached the thermal quasi-equilibrium state ($t \simeq 75\,ps$) as a function of $sin^2\theta/\lambda^2$ for several Bragg peaks.

Figure 4a) clearly shows that the loss of intensity of each Bragg reflection depends on the fluence and the norm of the wave vector, in agreement with thermal effects in diffraction theory. From the slope of the linear fits, it is possible to extract the temperature increase ΔT and the precise temperature of the quasi-equilibrium state called $T_{q.e.} = T_i + \Delta T$ in the following. The $T_{q.e.}$ temperatures have been obtained from the analysis of thirty Bragg reflections and are displayed in figure 4b) for several fluences and for the two initial temperatures (T_i =155 K and T_i =295 K). The $T_{q.e.}$ temperatures can also be estimated from the absorbed pump laser energy and is in good agreement with the results obtained from our Debye-Waller analysis (see figure 4b and Supplemental Material for details).

These results shows that the lattice temperature $T_{q.e.}$ never exceeds the critical temperature T_c, whatever the incident fluence and the initial temperature. However, we will see in the following that the CDW satellite reflections disappear above a threshold fluence proving that the photo-induced phase transition is athermal.

B. Dynamics of CDW satellite reflections and CDW recovery

The dynamics of the $2k_F$ reflection is very different from that of the Bragg peaks (see figure 5a). In order to enhance

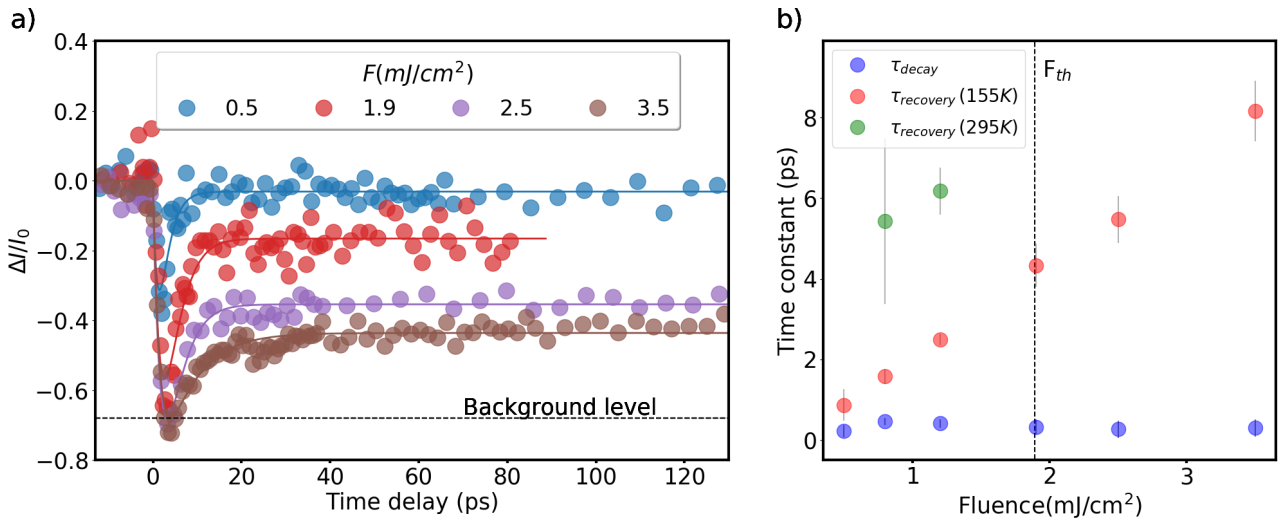

FIG. 5. a) Dots: satellite peaks' relative intensity changes for different incident fluences. Solid line: result of the double exponential fits b) Time constants extracted from the fits of a). Blue and red circles correspond to the decay and recovery time constants respectively, collected at a sample temperature of $T_i = 155$ K. Green circles corresponds to the recovery times collected at room temperature ($T_i = 295$ K).

the signal-to-noise ratio, each experimental point is an average over four satellite reflections with the same $|Q|$ value: $Q_{CDW} = (1, 0, \pm\delta)$ and $Q_{CDW} = (-1, 0, \pm\delta)$.

The intensity first abruptly drops with a characteristic temporal decay time τ_{decay} in less than a picosecond. Above the threshold fluence $F_{th} = 1.9\,mJ/cm^2$, the intensity of the satellite peaks is suppressed indicating an ultrafast suppression of the CDW order. The satellite peak intensity then increases again on a slower picosecond time scale with a recovery time $\tau_{recovery}$. Finally, at longer pump-probe delays, typically $t > 50$ ps, the intensity stays rather constant below the equilibrium intensity. This behavior is similar to that observed with Bragg peaks indicating that the system has reached a quasi-equilibrium state.

The temporal behavior can be well fitted using a double exponential function (see Supplementary Material) and the corresponding time constants are displayed in Figure 5b). The temporal decay τ_{decay} is typically less than 500 fs and was limited by the experimental resolution of our set-up. In order to get a better resolution, we used a shorter electron beam containing less charge and providing ~ 300 fs resolution instead of 1-1.5 ps, without being able to resolve the time decay whatever the fluence. This upper limit is in agreement with the previous time resolved X-ray diffraction experiment in which time decays of the order of ~ 200 fs as been reported by using a temporal resolution less than 80 fs in the similar $SmTe_3$ system[24].

The recovery time $\tau_{recovery}$ is well above the temporal resolution. For $T_i = 155$ K, the CDW recovery slows down linearly from 1 ps to 8 ps as the incident fluence is increased (see figure 5 b). At high fluences, the CDW recovery times $\tau_{recovery}$ and the Decay times $\tau_{thermal}$ of the Bragg peaks are similar, showing that the CDW is recovering while the lattice temperature is reaching the quasi-equilibrium temperature. For lower fluences, on the contrary, $\tau_{recovery}$ is smaller than $\tau_{thermal}$ meaning that the CDW recovery is carried out even before the main lattice is completely at the quasi-equilibrium state. This observation, along with the fact that the lattice temperature always remains below T_c, confirms the non-thermal nature of this out-of-equilibrium phase transition.

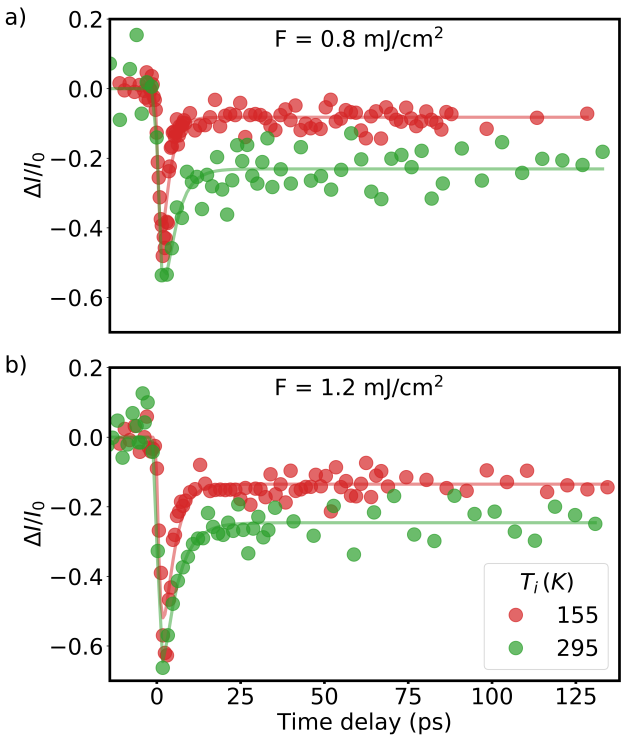

FIG. 6. Relative intensity changes of the satellite peaks at two different initial temperatures and two different fluences: a) at F = 0.8 mJ/cm^2 and b) at F = 1.2 mJ/cm^2.

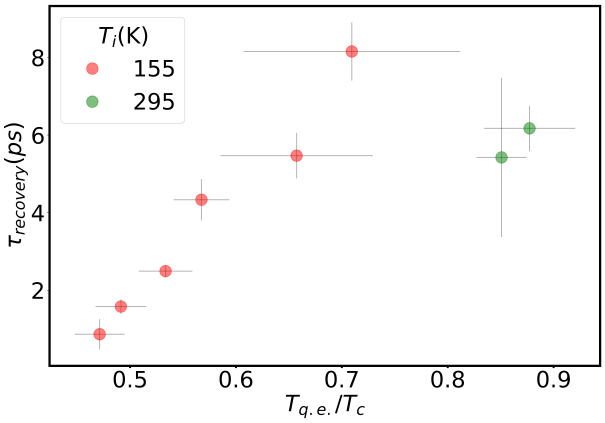

FIG. 7. Recovery time of the satellite reflections $\tau_{recovery}$ as a function of the quasi-equilibrium and critical temperatures ratio $T_{q.e.}/T_c$.

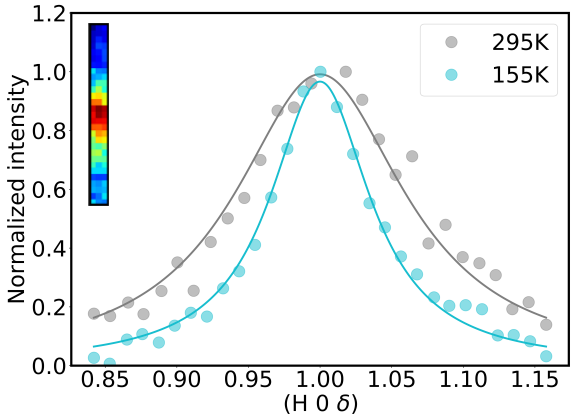

FIG. 8. Transverse profile along a^* of the (-10δ) satellite reflection at equilibrium (i.e. taken at negative time delays without pump) at $T_i = 155$ K (cyan) and at $T_i = 295$ K (gray). Inset: selected ROI around the satellite peak, the profile corresponds to the intensity integrated along the horizontal axis. The FWHM of the profile at $T_i = 155$ K has been considered as the resolution function of the instrument in the following ($\xi_r = 18 \cdot 10^{-3}$ Å^{-1}).

The temporal behavior of $GdTe_3$ is similar to the other RTe_3 compounds also observed by ultrafast electron diffraction[18,22]. In the present study, we investigate the effect of the initial temperature by measuring the dynamics starting with the two initial temperatures: $T_i = 155$ K and $T_i = 295$ K.

The lattice temperature increase is estimated from the dynamics of the Bragg peaks at $T_i = 295$ K following the same Debye-Waller analysis as in section III A. The result is again in good agreement with the temperatures estimated from heat absorption (see figure 4 b) and is similar for both initial temperatures: $\Delta T \sim 35$ K at F = 0.8 mJ/cm^2 and $\Delta T \sim 50$ K at F = 1.2 mJ/cm^2. Note that, in principle, the Debye-Waller factor should change with the initial temperature since phonon dispersion curves are temperature dependent especially at the $2k_F$ wave vector close to T_c. However, only low frequency acoustic modes located at the Brillouin zone center contribute to the Debye temperature which weakly vary in this temperature range. This low sensitivity of the temperature increase with respect to the initial temperature is therefore expected.

Contrary to Bragg reflections, the dynamics of the CDW satellites is clearly different for the two initial temperatures as shown in figures 5 b) and 6. Although the incident photoexcitation induces the same temperature increase for both initial temperatures, the CDW recovery is slower when the system is initially closer to T_c. The recovery times are almost 3 times larger at the higher initial temperature ($T_c - T_i =$ 82 K with T_i =295 K) than at the lower initial temperature ($T_c - T_i =$ 222 K with T_i =155 K). Futhermore, the slowing down is approximately linear versus fluences far from T_c (for T_i =155 K), while is compatible with a divergent recovery time closer to T_c, for T_i =295 K (see figure 5b where $\tau_{recovery}$=0 at $f = 0$) in agreement with pump-probe reflectivity in $TbTe_3$[38]. This point will be discussed later though the Rothwarf-Taylor (RT) model.

C. Loss of long-range order.

The CDW correlation length ξ can be retrieved from the satellite peak width in the diffraction patterns by taking $\xi = 1/FWHM$. Note that the peak width is not given by a rocking curve but results from a cut of the Ewald sphere convoluted by the experimental resolution leading to the largest correlation length measurable of 6.8 *nm*. Only the satellite profile along the transverse direction a^* is shown because the longitudinal profile along c^* is too much affected by the tails/wings of the Bragg peaks (see Fig. 1). The satellite profile along a^* is obtained by summing the intensity of a region of interest of 29×3 pixels containing the satellite reflection (see inset in figure 8) and the fit is performed by using a Pseudo-Voigt function plus a linear function that accounts for the background (see figure 5b)).

The complete dynamics of the FWHM in figure 9 a) clearly shows the loss of long-range order that appears after photoexcitation in the system. For $F > F_{th}$, the peak broadens significantly and does not relax to its initial width within the experimental temporal range. The stable FWHM reached at longer delays ($\tau_{thermal} \simeq 20$ ps) illustrates the smaller correlation length of the quasi equilibrium state. On the other hand, at low fluence, below the threshold value $F < F_{th}$, the FWHM shows small changes $\Delta w/w_0 < 8\%$, that quickly recover to the initial values (this low fluence case is limited by the experimental resolution). This behavior is clearly seen in figure 9 c).

As in the case of the intensity, the satellite width also depends on the initial temperature. Figure 8 clearly shows that the satellite peak width at equilibrium increases as the initial temperature approaches the critical temperature T_c. We find that the correlation length varies from $\xi = 6.8$ nm at

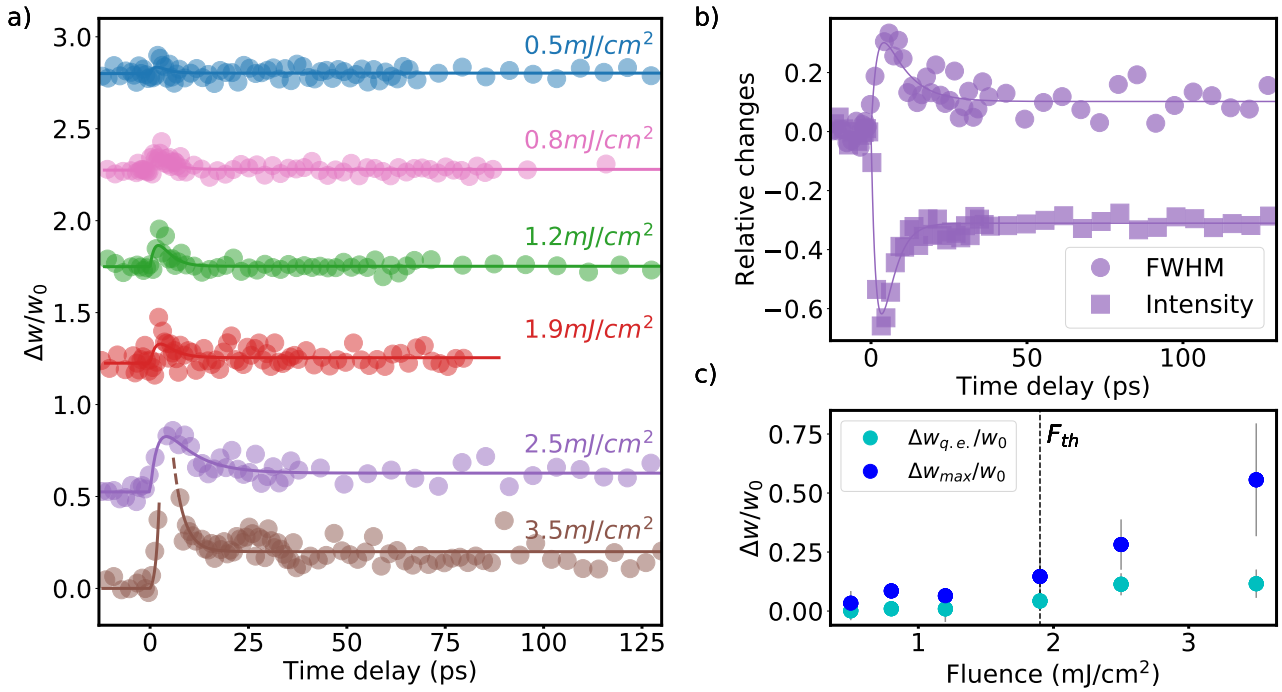

FIG. 9. a) Temporal evolution of $\Delta w/w_0$, the relative change of the peak FWHM for different incident fluences. The curves are vertically shifted for clarity. b) Relative intensity (squares) and FWHM (circles) temporal changes at an incident fluence of 2.5 mJ/cm^2, c) Relative changes of the FWHM maximum $\Delta w_{max}/w_0$ (averaged over the four points around the maximum) and after the time recovery at quasi-equilibrium $\Delta w_{q.e.}/w_0$ (averaged over the last twenty points of each curve in a)) where w_0 is the initial satellite width. Error bars represent the standard deviation derived from the average.

$T_i = 155$ K to $\xi = 4.2$ nm at $T_i = 295$ K.

Figure 9 b) displays on the same graph the temporal evolution of the FWHM and intensity of the satellite peak, showing that both observables display correlated dynamics, for both decay and recovery times. This behavior holds at all fluences and the recovery times of both intensity and FWHM increase linearly with incident fluence (see Supplementary Material).

D. No observation of a transient CDW phase along a

Previous UED work reported on the emergence of a transient "exotic" CDW state in $LaTe_3$[23] and $CeTe_3$[22] along the perpendicular a crystallographic axis. This state does not exist in the phase diagram at equilibrium and has only been observed in out-of-equilibrium conditions. Despite many attempts, we did not observed this transient CDW state in $GdTe_3$ at any accessible fluences. The satellite peaks might then be too weak in intensity, the transient phase might have a too short lifetime or simply does not exist. The absence of this phase could be linked to its quite different transition temperature. $GdTe_3$ displays a much lower critical temperature ($T_c \sim 377$ K) compared to $LaTe_3$ ($T_c \sim 670$ K) or $CeTe_3$ ($T_c \sim 540$ K) which means that the configuration space between the high temperature phase and the temperature of measurement is considerably reduced in $GdTe_3$ ($\Delta T = 82$ K) compared to $LaTe_3$ ($\Delta T = 375$ K) meaning that a small perturbation brings directly the system to its closest ground state in energy, the disordered phase.

IV. DISCUSSION

The temporal sequence of the photo-excitation and relaxation processes can be summarized as follows:

(1) electrons are first excited to higher energies in the conduction band and subsequently transfer their excess energy to hot phonons via electron-phonon coupling within the first picosecond following photo-excitation. Here, we do not directly detect high-energy phonons because of the limited temporal resolution, but previous time-resolved ARPES[39–41], transient reflectivity[18,42] and time-resolved X-ray diffraction[8,24] experiments have measured a coherent phonon corresponding to the amplitude mode, which oscillates at $\nu_{AM} \sim 2$ THz in RTe_3. At this stage, it is likely that the amplitude of the lattice periodic distortion is strongly suppressed along with an increase of disorder, in particular for higher fluences, $F > F_{th}$. **(2)** The lattice then thermalizes on a typical time scale $\tau_{thermal} \simeq 6$ ps. During this thermalization process, the lattice temperature increases, as can be inferred from Bragg peak intensity loss due to the Debye-Waller factor. Simultaneously, the CDW state recovers with a time scale $\tau_{recovery}$ that is faster than $\tau_{thermal}$ for $F < F_{th}$, slows down as the fluence is increased and saturates around $\tau_{thermal}$. The increase of the satellite width shows

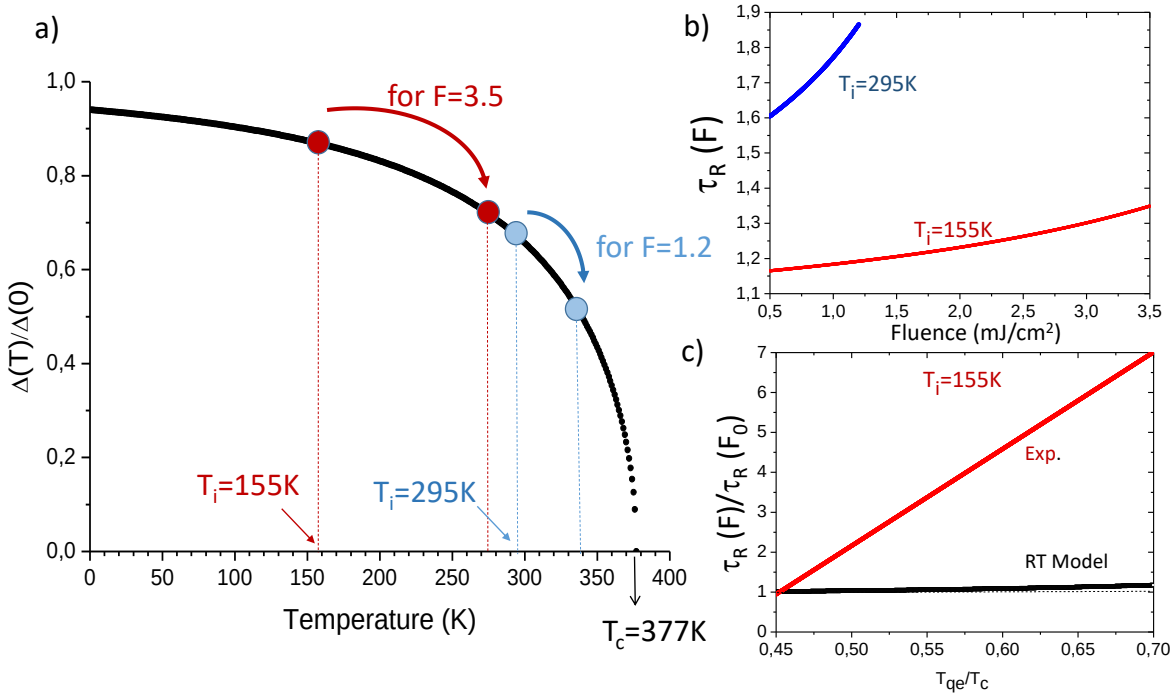

FIG. 10. a) Gap profile with fluences in the BCS theory for T_i=155K and T_i=295K. b) Overall behavior of $\tau_{recovery}$ with fluence for the two initial temperatures in the RT model. c) Comparison of $\tau_{recovery}(F)/\tau_{recovery}(F_0)$, where F_0=0.5mJ/cm^2 is the lowest fluence used in this study, between the experimental data and the RT model for T_i=155K.

that the dynamics is also affected by the phase ϕ of the order parameter.

(3) For $t \gg \tau_{thermal} \sim 6$ps, the system reaches a quasi-equilibrium state in which the lattice temperature stabilizes at the quasi-equilibrium temperature $T_{q.e.}$.

Let us now discuss the relevance of the Rothwarf-Taylor (RT) model in the case of CDWs, originally considered to describe the recombination lifetimes in superconductors, i.e. the time $\tau_{recovery}$ required for a quasiparticle at the gap edge to recombine with a thermally excited quasiparticle to form a Cooper pair[43]. In this approach, the recombination is inversely proportional to the gap:

$$\tau_{recovery}^{-1} = 12\Gamma_\omega k_B T' \Delta(T)/(\hbar\omega^2) \qquad (2)$$

where Γ_ω represents the Raman phonon linewidth and T' is the quasiparticle temperature. If we take into account the gap profile in the BCS theory,

$$\Delta(T) = \Delta(0)\tanh(1.74(1 - T_{qe}/T_c))$$

with $T_c = 377K$, and the measured T_{qe} from the Debye-Waller analysis, the gap versus the fluence can be obtained (see figure 10 a). The experimental recovery time can then be compared to the RT theory for the two initial temperatures. In the RT model, the recombination time is much larger for initial temperature closer to T_c (see figure 10 b). This is in agreement with the present data and with pump-probe reflectivity observing divergent τ_R close to T_c[38,42]. However, the agreement remains only qualitative. If we consider that $\tau_{recovery}(F)$ is mainly driven by $\Delta(F)$ in the eq. 2, the other variables Γ_ω, T' and ω varying less in this temperature range, the ratio $\tau_{recovery}(F)/\tau_{recovery}(F_0) = \Delta(F_0)/\Delta(F)$ can be compared to the experiment. As shown in figure 10 c), the experiment strongly differs from the theory. The observed recovery time is much larger than expected. Even if the gap obviously plays a crucial role in the slowing down close to T_c, explaining the overall $\tau_{recovery}$ behavior, the model underestimate the slowing down.

This underestimation can be justified by several arguments. We can first observe that the gap profile in figure 10a) results from a mean-field approach at equilibrium which is far from being the case here. We can also question the use of the RT model, initially intended to describe superconductivity and transferred to CDW systems. In particular, phonons in the Peierls transition are associated to soft modes close to T_c. However, the influence of defects, obviously not considered in the RT model, could strongly slow down the process. The origin of the slower relaxation can indeed be assigned to disorder, illustrated here by the loss of long-range order when T_i approaches T_c. The decreasing phase-phase correlation function, leading to increasing satellite width (see figure 9b), can be induced by lattice strain or/and CDW dislocations[44,45]. As an example, the $GdTe_3$ atomic structure displays weak interactions between pure Te layers. The laser pulse may induce certain strain along the *b* crystallographic axis (perpendicular to the Te nets containing the CDW) and perturb the CDW reformation. However, a detailed analysis of the positions of

all Bragg peaks did not reveal any lattice changes along b^* considering our spatial resolution.

V. CONCLUSION

We presented a detailed experimental study of the CDW dynamics in $GdTe_3$. Our ultrafast electron diffraction results show that the pump laser pulse is able to trigger a non-thermal photo-induced phase transition which occurs for lattice temperatures below T_c in out-of-equilibrium conditions. The CDW is found to be suppressed in the disordered state following photo-excitation for large enough fluences ($F > F_{th} = 1.9$ mJ/cm^2). We observed that the CDW state recovers while the lattice is thermalizing on time scale $\tau_{thermal} \simeq 6$ ps. The CDW recovery is found to be increasing with the incident fluence and the initial sample temperature. The slowing down of the CDW recovery was closely related to the temperature in the quasi-equilibrium state $T_{q.e.}$.

Our results are consistent with recent results obtained in other materials of the RTe_3 family[18,22]. In particular, we also observe a broadening of the CDW satellite peaks, and confirm the loss of long-range order with underestimated time recombination. Our results performed at different initial temperatures showed that the slowing down in the CDW relaxation is greatly influenced by the lattice temperature.

Future diffraction experiments investigating more systematically the effect of the initial temperature should allow us to better understand its role in the observed dynamics. In addition, experiments with a THz pump could potentially reduce lattice heating induced by the infrared pump pulse and allow to discriminate better the respective role of temperature and pump fluence in the dynamics of this out-of-equilibrium phase transition.

ACKNOWLEDGMENTS

This work was funded by the European Research Council under Contract No. 306708, ERC Starting Grant FEMTOELEC, supported by "Investissements d'Avenir" LabEx PALM (ANR-10-LABX-0039-PALM), and Laserlab-Europe (EUH2020 654148). The authors are thankfull to P. Lejay (Institut Néel, CNRS and Université Joseph Fourier, BP166, 38042 Grenoble, France) for sample growth." We also acknowledge fruitful discussions with Dr. S. Ravy and Prof. Luca Perfetti.

[1] J. Chang, E. Blackburn, A. T. Holmes, N. B. Christensen, J. Larsen, J. Mesot, R. Liang, D. A. Bonn, W. N. Hardy, A. Watenphul, M. V. Zimmermann, E. M. Forgan, and S. M. Hayden, "Direct observation of competition between superconductivity and charge density wave order in $YBa_2Cu_3O_{6.67}$," Nat. Phys. **8**, 871–876 (2012).

[2] S. Blanco-Canosa, A. Frano, T. Loew, Y. Lu, J. Porras, G. Ghiringhelli, M. Minola, C. Mazzoli, L. Braicovich, E. Schierle, E. Weschke, M. Le Tacon, and B. Keimer, "Momentum-Dependent Charge Correlations in $YBa_2Cu_3O_{6+\delta}$ Superconductors Probed by Resonant X-Ray Scattering: Evidence for Three Competing Phases," Phys. Rev. Lett. **110**, 187001 (2013).

[3] G. Grüner, *Density Waves in Solids*, Advanced book program: Addison-Wesley (Perseus Books Group, 2000).

[4] M. D. Johannes, I. I. Mazin, and C. A. Howells, "Fermi-surface nesting and the origin of the charge-density wave in $NbSe_2$," Phys. Rev. B **73**, 205102 (2006).

[5] M. D. Johannes and I. I. Mazin, "Fermi surface nesting and the origin of charge density waves in metals," Phys. Rev. B **77**, 165135 (2008).

[6] V. Brouet, W. L. Yang, X. J. Zhou, Z. Hussain, R. G. Moore, R. He, D. H. Lu, Z. X. Shen, J. Laverock, S. B. Dugdale, N. Ru, and I. R. Fisher, "Angle-resolved photoemission study of the evolution of band structure and charge density wave properties in RTe$_3$ (R = Y, La, Ce, Sm, Gd, Tb, and Dy)," Phys. Rev. B **77**, 235104 (2008).

[7] K. Rossnagel, "On the origin of charge-density waves in select layered transition-metal dichalcogenides," J. Phys.: Condens. Matter **23**, 213001 (2011).

[8] T. Huber, S. O. Mariager, A. Ferrer, H. Schäfer, J. A. Johnson, S. Grübel, A. Lübcke, L. Huber, T. Kubacka, C. Dornes, C. Laulhe, S. Ravy, G. Ingold, P. Beaud, J. Demsar, and S. L. Johnson, "Coherent structural dynamics of a prototypical charge-density-wave-to-metal transition," Phys. Rev. Lett. **113** (2014).

[9] R. G. Moore, W. S. Lee, P. S. Kirchman, Y. D. Chuang, A. F. Kemper, M. Trigo, L. Patthey, D. H. Lu, O. Krupin, M. Yi, D. A. Reis, D. Doering, P. Denes, W. F. Schlotter, J. J. Turner, G. Hays, P. Hering, T. Benson, J. H. Chu, T. P. Devereaux, I. R. Fisher, Z. Hussain, and Z. X. Shen, "Ultrafast resonant soft x-ray diffraction dynamics of the charge density wave in $TbTe_3$," Phys. Rev. B **93**, 024304 (2016).

[10] W. S. Lee, Y. D. Chuang, R. G. Moore, Y. Zhu, L. Patthey, M. Trigo, D. H. Lu, P. S. Kirchmann, O. Krupin, M. Yi, M. Langner, N. Huse, J. S. Robinson, Y. Chen, S. Y. Zhou, G. Coslovich, B. Huber, D. A. Reis, R. A. Kaindl, R. W. Schoenlein, D. Doering, P. Denes, W. F. Schlotter, J. J. Turner, S. L. Johnson, M. Först, T. Sasagawa, Y. F. Kung, A. P. Sorini, A. F. Kemper, B. Moritz, T. P. Devereaux, D. H. Lee, Z. X. Shen, and Z. Hussain, "Phase fluctuations and the absence of topological defects in a photo-excited charge-ordered nickelate," Nat. Commun. **3** (2012).

[11] T.-r. T. Han, Z. Tao, S. D. Mahanti, K. Chang, C.-y. Ruan, C. D. Malliakas, and M. G. Kanatzidis, "Structural dynamics of two-dimensional charge-density waves in $CeTe_3$ investigated by ultrafast," Phys. Rev. B **86**, 075145 (2012).

[12] P. Beaud, S. L. Johnson, E. Vorobeva, U. Staub, R. A. De Souza, C. J. Milne, Q. X. Jia, and G. Ingold, "Ultrafast structural phase transition driven by photoinduced melting of charge and orbital order," Phys. Rev. Lett. **103**, 155702 (2009).

[13] N. Erasmus, M. Eichberger, K. Haupt, I. Boshoff, G. Kassier, R. Birmurske, H. Berger, J. Demsar, and H. Schwoerer, "Ultrafast Dynamics of Charge Density Waves in 4H$_b$-$TaSe_2$ Probed by Femtosecond Electron Diffraction," Phys. Rev. Lett. **109**, 167402 (2012).

[14] K. Haupt, M. Eichberger, N. Erasmus, A. Rohwer, J. Demsar, K. Rossnagel, and H. Schwoerer, "Ultrafast Metamorphosis of a Complex Charge-Density Wave," Phys. Rev. Lett. **116**, 016402 (2016).

[15] C. Laulhé, T. Huber, G. Lantz, A. Ferrer, S. O. Mariager, S. Grübel, J. Rittmann, J. A. Johnson, V. Esposito, A. Lübcke, L. Huber, M. Kubli, M. Savoini, V. L. R. Jacques, L. Cario, B. Corraze, E. Janod, G. Ingold, P. Beaud, S. L. Johnson, and S. Ravy, "Ultrafast Formation of a Charge Density Wave State in 1T-TaS_2 : Observation at Nanometer Scales Using Time-Resolved X-Ray Diffraction," Phys. Rev. Lett. **118**, 247401 (2017).

[16] A. Singer, S. K. K. Patel, R. Kukreja, V. Uhlíř, J. Wingert, S. Festersen, D. Zhu, J. M. Glownia, H. T. Lemke, S. Nelson, M. Kozina, K. Rossnagel, M. Bauer, B. M. Murphy, O. M. Magnussen, E. E. Fullerton, and O. G. Shpyrko, "Photoinduced enhancement of the charge density wave amplitude," Phys. Rev. Lett. **117**, 056401 (2016).

[17] V. L. R. Jacques, C. Laulhé, N. Moisan, S. Ravy, and D. Le Bolloc'h, "Laser-induced charge-density-wave transient depinning in chromium," Phys. Rev. Lett. **117**, 156401 (2016).

[18] A. Zong, A. Kogar, Y. Q. Bie, T. Rohwer, C. Lee, E. Baldini, E. Ergeçen, M. B. Yilmaz, B. Freelon, E. J. Sie, H. Zhou, J. Straquadine, P. Walmsley, P. E. Dolgirev, A. V. Rozhkov, I. R. Fisher, P. Jarillo-Herrero, B. V. Fine, and N. Gedik, "Evidence for topological defects in a photoinduced phase

transition," Nat. Phys. **15**, 27–31 (2019).
[19]R. Yusupov, T. Mertelj, V. V. Kabanov, S. Brazovskii, P. Kusar, J. H. Chu, I. R. Fisher, and D. Mihailovic, "Coherent dynamics of macroscopic electronic order through a symmetry breaking transition," Nat. Phys. **6**, 681–684 (2010).
[20]T. Mertelj, P. Kusar, V. V. Kabanov, P. Giraldo-Gallo, I. R. Fisher, and D. Mihailovic, "Incoherent topological defect recombination dynamics in $TbTe_3$," Phys. Rev. Lett. **110**, 1–5 (2013).
[21]S. Vogelgesang, G. Storeck, J. G. Horstmann, T. Diekmann, M. Sivis, S. Schramm, K. Rossnagel, S. Schäfer, and C. Ropers, "Phase ordering of charge density waves traced by ultrafast low-energy electron diffraction," Nat. Phys. **14**, 184–190 (2017).
[22]F. Zhou, J. Williams, S. Sun, C. D. Malliakas, M. G. Kanatzidis, A. F. Kemper, and C.-Y. Ruan, "Nonequilibrium dynamics of spontaneous symmetry breaking into a hidden state of charge-density wave," Nat. Commun. , 566 (2021).
[23]A. Kogar, A. Zong, P. E. Dolgirev, X. Shen, J. Straquadine, Y. Q. Bie, X. Wang, T. Rohwer, I. C. Tung, Y. Yang, R. Li, J. Yang, S. Weathersby, S. Park, M. E. Kozina, E. J. Sie, H. Wen, P. Jarillo-Herrero, I. R. Fisher, X. Wang, and N. Gedik, "Light-induced charge density wave in $LaTe_3$," Nat. Phys. **16**, 159–163 (2020).
[24]M. Trigo, M. E. Kozina, T. Henighan, M. P. Jiang, H. Liu, J. N. Clark, M. Chollet, J. M. Glownia, D. Zhu, T. Katayama, D. Leuenberger, P. S. Kirchmann, I. R. Fisher, Z. X. Shen, and D. A. Reis, "Coherent order parameter dynamics in $SmTe_3$," Phys. Rev. B **99**, 104111 (2019).
[25]A. Cavalleri, C. Tóth, C. W. Siders, J. A. Squier, F. Ráksi, P. Forget, and J. C. Kieffer, "Femtosecond Structural Dynamics in VO_2 during an Ultrafast Solid-Solid Phase Transition," Phys. Rev. Lett. **87**, 237401 (2001).
[26]E. Collet, M.-H. Lemée-Cailleau, M. Buron-Le Cointe, H. Cailleau, M. Wulff, T. Luty, S.-Y. Koshihara, M. Meyer, L. Toupet, P. Rabiller, and S. Techert, "Laser-Induced Ferroelectric Structural Order in an Organic Charge-Transfer Crystal," Science **300**, 612–615 (2003).
[27]N. Gedik, D.-S. Yang, G. Logvenov, I. Bozovic, and A. H. Zewail, "Nonequilibrium Phase Transitions in Cuprates Observed by Ultrafast Electron Crystallography," Science **316**, 425–429 (2007).
[28]V. R. Morrison, R. P. Chatelain, K. L. Tiwari, A. Hendaoui, A. Bruhács, M. Chaker, and B. J. Siwick, "A photoinduced metal-like phase of monoclinic VO_2 revealed by ultrafast electron diffraction," Science **346**, 445–448 (2014).
[29]N. Ru and I. R. Fisher, " Thermodynamic and transport properties of YTe_3 , $LaTe_3$, and $CeTe_3$," Phys. Rev. B **73**, 033101 (2006).
[30]d. L. M. van der Geer, S.B., "Pulsar physics and the general particle tracer (gpt) code," `http://www.pulsar.nl/gpt`.
[31]N. Ru, C. L. Condron, G. Y. Margulis, K. Y. Shin, J. Laverock, S. B. Dugdale, M. F. Toney, and I. R. Fisher, "Effect of chemical pressure on the charge density wave transition in rare-earth tritellurides RTe_3," Phys. Rev. B **77**, 035114 (2008).
[32]C. Malliakas, S. J. L. Billinge, H. J. Kim, and M. G. Kanatzidis, "Square Nets of Tellurium: Rare-Earth Dependent Variation in the Charge-Density Wave of $RETe_3$ (RE = Rare-Earth Element)," J. Am. Chem. Soc. **127**, 6510–6511 (2005).
[33]C. D. Malliakas and M. G. Kanatzidis, "Divergence in the Behavior of the Charge Density Wave in $RETe_3$ (RE = Rare-Earth Element) with Temperature and RE Element," J. Am. Chem. Soc. **128**, 12612–12613 (2006).
[34]N. Ru, *Charge Density Wave formation in Rare-Earth Tritellurides*, Ph.D. thesis, Stanford University (2008).
[35]A. A. Sinchenko, P. Lejay, and P. Monceau, "Sliding charge-density wave in two-dimensional rare-earth tellurides," Phys. Rev. B **85**, 241104 (2012).
[36]E. DiMasi, M. C. Aronson, J. F. Mansfield, B. Foran, and S. Lee, "Chemical pressure and charge-density waves in rare-earth tritellurides," Phys. Rev. B **52**, 14516–14525 (1995).
[37]J. Als-Nielsen and D. McMorrow, *Elements of Modern X-ray Physics* (John Wiley & Sons, Ltd, 2011).
[38]R. Y. Chen, B. F. Hu, T. Dong, and N. L. Wang, "Revealing multiple charge-density-wave orders in $TbTe_3$ by optical conductivity and ultrafast pump-probe experiments," Phys. Rev. B **89**, 075114 (2014).
[39]F. Schmitt, P. S. Kirchmann, U. Bovensiepen, R. G. Moore, M. K. L. Rettig, J.-H. Chu, N. Ru, L. Perfetti, D. H. Lu, M. Wolf, I. R. Fisher, and Z.-X. Shen, "Transient Electronic Structure and Melting of a Charge Density Wave in $TbTe_3$," Science **321**, 1649 (2008).
[40]D. Leuenberger, J. A. Sobota, S. Yang, A. F. Kemper, R. G. Moore, I. R. Fisher, P. S. Kirchmann, T. P. Devereaux, and Z. Shen, "Classification of collective modes in a charge density wave by momentum-dependent modulation of the electronic band structure," Phys. Rev. B **91**, 201106(R) (2015).
[41]L. Rettig, R. Cortés, J. H. Chu, I. R. Fisher, F. Schmitt, R. G. Moore, Z. X. Shen, P. S. Kirchmann, M. Wolf, and U. Bovensiepen, "Persistent order due to transiently enhanced nesting in an electronically excited charge density wave," Nat. Commun. **7**, 10459 (2016).
[42]R. V. Yusupov, T. Mertelj, J.-H. Chu, I. R. Fisher, and D. Mihailovic, "Single-Particle and Collective Mode Couplings Associated with 1- and 2-Directional Electronic Ordering in Metallic RTe_3 (R = Ho, Dy, Tb)," Phys. Rev. Lett. **101**, 246402 (2008).
[43]A. Rothwarf and B. N. Taylor, "Measurement of recombination lifetimes in superconductors," Phys. Rev. Lett. **19**, 27–30 (1967).
[44]S. Brazovskii, C. Brun, Z.-Z. Wang, and P. Monceau, "Scanning-tunneling microscope imaging of single-electron solitons in a material with incommensurate charge-density waves," Phys. Rev. Lett. **108**, 096801 (2012).
[45]D. Le Bolloc'h, S. Ravy, J. Dumas, J. Marcus, F. Livet, C. Detlefs, F. Yakhou, and L. Paolasini, "Charge density wave dislocation as revealed by coherent x-ray diffraction," Phys. Rev. Lett. **95**, 116401 (2005).